Acta Oceanol. Sin., 2017, Vol. 36, No. 5, P. 1–8
DOI: 10.1007/s13131-017-1057-4
http://www.hyxb.org.cn
E-mail: hyxbe@263.net

A fresh look at the deepwater overflow in the Luzon Strait

ZHU Yaohua[1, 2], SUN Junchuan[1, 2], WEI Zexun[1, 2*], WANG Yonggang[1, 2], FANG Guohong[1, 2], QU Tangdong[3]

[1] Key Laboratory of Marine Science and Numerical Modeling, The First Institute of Oceanography, State Oceanic Administration, Qingdao 266061, China

[2] Laboratory for Regional Oceanography and Numerical Modeling, Qingdao National Laboratory for Marine Science and Technology, Qingdao 266071, China

[3] Joint Institute for Regional Earth System Science and Engineering, University of California, Los Angeles 90095, USA

Received 6 December 2016; accepted 17 January 2017

Abstract

On the basis of the latest version of a U.S. Navy generalized digital environment model (GDEM-V3.0) and World Ocean Atlas (WOA13), the hydraulic theory is revisited and applied to the Luzon Strait, providing a fresh look at the deepwater overflow there. The result reveals that: (1) the persistent density difference between two sides of the Luzon Strait sustains an all year round deepwater overflow from the western Pacific to the South China Sea (SCS); (2) the seasonal variability of the deepwater overflow is influenced not only by changes in the density difference between two sides of the Luzon Strait, but also by changes in its upstream layer thickness; (3) the deepwater overflow in the Luzon Strait shows a weak semiannual variability; (4) the seasonal mean circulation pattern in the SCS deep basin does not synchronously respond to the seasonality of the deepwater overflow in the Luzon Strait. Moreover, the deepwater overflow reaches its seasonal maximum in December (based on GDEM-V3.0) or in fall (October–December, based on the WOA13), accompanied by the lowest temperature of the year on the Pacific side of the Luzon Strait. The seasonal variability of the deepwater overflow is consistent with the existing longest (3.5 a) continuous observation along the major deepwater passage of the Luzon Strait.

Key words: Luzon Strait, deepwater overflow, seasonal variability, South China Sea

Citation: Zhu Yaohua, Sun Junchuan, Wei Zexun, Wang Yonggang, Fang Guohong, Qu Tangdong. 2017. A fresh look at the deepwater overflow in the Luzon Strait. Acta Oceanologica Sinica, 36(5): 1–8, doi: 10.1007/s13131-017-1057-4

1 Introduction

The Luzon Strait, with its deepest sill at about 2 400 m (Smith and Sandwell, 1997), is the only passage of deepwater renewal of the South China Sea (SCS). The deepwater exchange through the Luzon Strait has a decisive influence on the deep circulation, deepwater renewal, and heat and salt fluxes of the SCS. By comparison of density profiles between two sides of the Luzon Strait based on the World Ocean Database 2001, Qu et al. (2006) reveal that there are two bifurcations in the long-term mean potential density profiles. Specifically, the upper bifurcation occurs at depth of 81 m, and the lower bifurcation at 1 489 m. Water on the Pacific side is of higher density than that on the SCS side above the upper bifurcation and below the lower bifurcation. Below the lower bifurcation (hereinafter referred to as the bifurcation), the density difference between two sides of the Luzon Strait yields a baroclinic pressure head driving the deepwater overflow from the western Pacific to the SCS. With existing *in situ* observations, theoretical analyses, and numerical modeling, it has been accepted that water flows persistently from the western Pacific into the SCS through the deep channel of the Luzon Strait (e.g., Wyrtki, 1961; Nitani et al., 1972; Wang, 1986; Qu et al., 2000, 2006; Tian et al., 2006; Fang et al., 2009; Yang et al., 2010; Zhang et al., 2010, 2015; Xu and Oey, 2014; Zhao et al., 2014; Zhou et al., 2014). In particular, Qu et al. (2006) applied the hydraulic theory developed by Whitehead (1989, 1998) to the Luzon Strait. Their analysis yielded a transport of 2.5×10^6 m^3/s, which has been used as an upper bound estimate of the Luzon Strait deepwater overflow. But, the seasonality of this deepwater overflow remains poorly understood.

Following Qu et al. (2006), a couple of studies recently proposed a seasonal variability of the deepwater overflow but reached opposite conclusions. Zhao et al. (2014) used the hydraulic theory to study the seasonal variability of the deepwater overflow in the Luzon Strait, based on the result from a high resolution hybrid coordinate ocean model (HYCOM). They found that the density difference between the Pacific and SCS sides at the averaged sill depth of the Luzon Strait is greater in winter (0.085 kg/m^3) than in summer (0.079 kg/m^3). By assuming a constant bifurcation depth at 1 450 m, they conclude that the Luzon Strait deepwater overflow is stronger in winter (3.6×10^6 m^3/s) and weaker in summer (3.3×10^6 m^3/s). Afterwards, Lan et al. (2015) calculated the monthly mean potential density averaged on both

Foundation item: The National Natural Science Foundation of China (NSFC)—Shandong Joint Fund for Marine Science Research Centers of China under contract No. U1606405; the National Basic Research Program (973 Program) of China under contract No. 2011CB403502; the National High Technology Research and Development Program (863 Program) of China under contract No. 2013AA09A506; the National Program on Global Change and Air-Sea Interaction under contract Nos GASI-IPOVAI-01-02 and GASI-03-01-01-04; the National Natural Science Foundation of China under contract No. 41606040.
*Corresponding author, E-mail: weizx@fio.org.cn

sides of the Luzon Strait based on the simple ocean data assimilation (SODA2.1.6) outputs. They illustrated the density difference between two sides of the Luzon Strait at the 1 500 m depth, from under 0.025 kg/m^3 before July to its seasonal maximum of about 0.033 kg/m^3 in November. Their density difference at the 1 500 m depth is significantly smaller than that of Zhao et al. (2014) at the averaged sill depth (2 181 m) of the Luzon Strait. According to Lan et al. (2015), the Luzon Strait deepwater overflow varies corresponding to the deep circulation in the SCS, specifically, stronger in summer and weaker in winter. This seasonality is just opposite to the numerical result of Zhao et al. (2014).

The existing longest direct measurement of the deepwater overflow in the Luzon Strait, as we are aware of, is 3.5 a continuous mooring observations conducted in the deep Bashi Channel and the Luzon Trough from October 2009 to April 2013 (Zhou et al., 2014). According to their observations, the density difference between two sides of the Luzon Strait is larger in winter, which supposes to drive a stronger deepwater overflow than in summer. However, it cannot explain the seasonality of their observed along channel velocity, which is intensified in October–December (hereinafter referred to as fall corresponding to the WOA dataset) rather than in winter.

Owing to the major discrepancies among the previous studies, it becomes necessary and highly desirable to revisit the hydraulic theory and provide a more complete understanding of the seasonality of the deepwater overflow and its related ocean dynamics in the Luzon Strait. In fact, taking a closer inspection of the monthly or seasonal density profiles on both sides of the Luzon Strait, one can find that not only the density difference but also the bifurcation depth is seasonally varying. If the bifurcation depth or the thickness of the deepwater overflow varies, the transport of the deepwater overflow varies too. However, by assuming a constant bifurcation depth, this impact on the seasonal variability of the deepwater overflow was ignored in the previous studies. On the other hand, since the previous studies applied hydraulic theory to the deepwater overflow in the Luzon Strait based either on model results (Lan et al., 2015; Zhao et al., 2014) or on the coarse-resolution hydrographic dataset (WOA01), it seems favorable to address this issue by using comparatively high resolution and up to date hydrographic datasets. In this study, both newly-structured observation-based hydrographic model data and the most complete observational hydrographic data are analyzed to achieve consistent conclusions and provide a fresh understanding of the seasonality of the Luzon Strait deepwater overflow. Specifically, the U.S. Navy generalized digital environment model (GDEM) (Teague et al., 1990) has recently been updated as the version GDEM-V3.0 to provide a new temperature and salinity climatology (Carnes, 2009). According to Teague et al. (1990), both GDEM and WOA can similarly describe the large-scale oceanographic features, but the GDEM appears to render better representations of the seasonal variability and regions of high current shear because of a different smoothing method and a finer-grid spacing. Meanwhile, the National Oceanographic Data Center (NODC) of U.S. National Oceanic and Atmospheric Administration (NOAA) has also upgraded the WOA09 dataset to WOA13 (Boyer et al., 2014). The latest versions of both datasets are eagerly expected to present comparatively reliable potential density profiles for describing the unknown seasonality of the Luzon Strait deepwater overflow.

The main objective of this study is to contrast the relative importance between the thickness of the deepwater overflow and the density difference between two sides of the Luzon Strait, and reveal the seasonal variability of the deepwater overflow based on the latest versions of the GDEM and the WOA, as well as verify the response of the deep SCS circulation to the deepwater overflow in the Luzon Strait. The data and method of analysis are briefly described in Section 2. Results are presented in Section 3, followed by a summary and discussion in Section 4.

2 Data and method of analysis

2.1 *GDEM-V3.0*

In the GDEM-V3.0, the gridded ocean temperature and salinity data have been generated by 4.5×10^6 observed T-S profiles dating back to 1920. The monthly climatology of the temperature and salinity is distinctively truncated to three decimal places (0.001 precision), with a horizontal resolution of 0.25°×0.25° and 78 vertical levels from the sea surface to 6 600 m. The denser vertical layers of the GDEM-V3.0 are conducive to reflect more accurate density profiles than those of coarse resolution models in the deepwater. The GDEM-V3.0 has been improved greatly in comparison with its earlier versions (e.g., GDEM-V2.6). The major difference is that GDEM-V3.0 horizontally interpolates temperature and salinity separately at each depth level instead of fitting temperature profiles to a prescribed nonlinear function. The improved gridding algorithm and eliminated interpolation across land boundaries describe temperature and salinity fronts much better along land the boundaries at each depth. A vertical gradient correction is employed to reduce the bias and improve the vertical gradients in the averaged profiles (Carnes, 2009), which could be an important benefit to this work.

2.2 *WOA13*

The monthly climatology of the observed temperature and salinity in the WOA13 dataset only covers 1 500 m of depth in the ocean. In order to investigate the Luzon Strait deepwater overflow, which exists below the depth of 1 500 m, we choose the seasonal climatology of the temperature and salinity. The seasonal climatology of the temperature and salinity with a horizontal resolution of 0.25°×0.25° and 102 vertical levels from the sea surface to 5 500 m has been markedly improved compared with the previous WOA versions with 1° horizontal resolution and 33 standard depth levels. The latest version of the GDEM and WOA datasets with finer resolution are conducive to describe the seasonal density structure of the Luzon Strait deepwater (Table 1).

The deepwater overflow in the Luzon Strait is driven by the inhomogeneous density distribution between the two sides of the strait. To accurately describe the water density in the upstream and downstream of the Luzon Strait, we use two 1°×1°square areas to collect and average the temperature and salinity. The square area A (21°–22°N, 122°–123°E) is just located near the eastern tip of the Bashi Channel to represent the upstream area of the Luzon Strait (i.e., the western Pacific side), while square area B (20°–21°N, 120°–121°E) is located near the southwest end of the Luzon Trough to stand for the downstream area of the Luzon Strait (i.e., the SCS side) (Fig. 1). The density difference between the two sides of the Luzon Strait, hereinafter, indicates the density averaged in Area A minus the density averaged in Area B.

2.3 *Application of hydraulic theory*

On the basis of the hydraulic theory, the maximum volume transport Q through a deep passage can be estimated as follows (readers are directed to Whitehead (1989, 1998) and Qu et al. (2006)):

Table 1. Comparison of data sources

Data	Version	Source	Climatology	Resolution	Vertical level	Deepest level/m
GDEM-V2.6	earlier	model	monthly	0.5°×0.5°	35	5 500
GDEM-V3.0	latest	model	monthly	0.25°×0.25°	78	6 600
WOA09	earlier	observation	seasonally	1°×1°	33	5 500
WOA13	latest	observation	seasonally	0.25°×0.25°	102	5 500

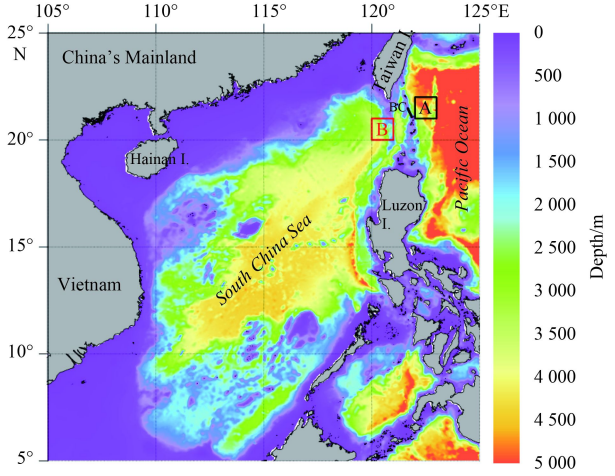

Fig. 1. Bottom topography of the South China Sea (Smith and Sandwell, 1997). The square area A (21°–22°N, 122°–123°E) and B (20°–21°N, 120°–121°E) represent the Pacific side (upstream) and South China Sea side (downstream) of the Luzon Strait respectively. The black line marked "BC" indicates the sill section of the Bashi Channel at the eastern tip, with its average depth of 2 181 m along this section.

$$Q = \frac{g' h_u^2}{2f} \quad \text{when } L > \frac{(2g'h_u)^{1/2}}{f}, \tag{1}$$

where $g'=g\Delta\rho/\rho$, g is the gravitational acceleration, ρ and $\Delta\rho$ are the characteristic density of deepwater and the maximum water density difference between the upstream and downstream of the passage; f is the Coriolis parameter; L is the width of the passage at the bifurcation depth; h_u is the upstream fluid interface height above the averaged sill (i.e., the upstream layer thickness of the deepwater overflow) in the Bashi Channel; and $(2g'h_u)^{1/2}/f$ is the Rossby radius. According to Whitehead (1998), the density difference used in Eq. (1) is the maximum value of the density difference between the upstream and downstream of the deepwater passage, occurring at any depth from the bifurcation to the sill. In this study, the density difference between Areas A and B increases with depth from the bifurcation to the averaged sill. Thus, the maximum density difference equals the density difference at the averaged sill depth (Fig. 2). With the definitions given by Whitehead (1998), based on the WOA13 climatological data, we have the mean bifurcation depth of 1 439 (m), h_u=2 181–1 439=742 (m), and the maximum density difference $\Delta\rho$=0.061 1 kg/m^3, thus the Rossby radius r=17.8 km when the Coriolis parameter is used at 21°N in the Bashi Channel. According to Smith and Sandwell's (1997), at the bifurcation depth, the width of sill section in the Bashi Channel is a little wider than 0.2° latitude (i.e., 22.2 km), which is slightly greater than the Rossby radius of 17.8 km. Therefore, the case for wide channel applies. From Eq. (1), we can see that the volume transport Q depends on the upstream layer thickness h_u and density difference $\Delta\rho$, which are a seasonal variable as demonstrated in the following section.

3 Seasonality of deepwater overflow

3.1 *A brief review of climatological mean potential density*

Figure 2a shows a gradually increasing density difference with depth below the bifurcation based on the WOA13. The maximum density difference between Areas A and B is 0.061 1 kg/m^3 occurring at the average sill depth. According to Eq. (1), the climatological mean deepwater overflow is estimated to be 3.04×10^6 m^3/s.

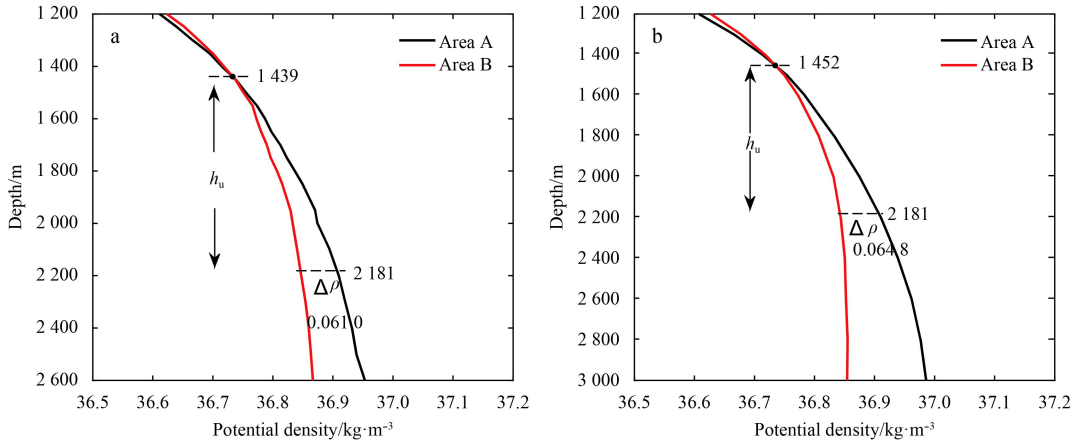

Fig. 2. Annual mean potential density profiles based on WOA13 (a) and GDEM-V3.0 (b) averaged in Areas A and B.

On the other hand, based on the GDEM-V3.0, Fig. 2b illustrates the climatological mean potential density profiles of the both sides of the Luzon Strait, showing that below the bifurcation depth of 1 452 m water on the Pacific side is of higher density than water on the SCS side. Resulting from the well stratified north Pacific water and the relatively homogeneous SCS water in the deep layer, the density difference yields a pressure head that drives a westward deepwater overflow into the SCS above the

Luzon Strait sill. With the maximum density difference of 0.064 8 kg/m^3 and h_u=729 m, the climatological mean deepwater overflow is estimated to be 3.1×10^6 m^3/s, indicating a highly consistent estimate with that from the WOA13. This magnitude of transport is coincident with the boundary current transport below 2 400 m in the SCS estimated by Wang et al. (2011), specifically, 3.13×10^6 m^3/s of westward transport through the northern boundary of 117°E section, 2.92×10^6 m^3/s of southward transport through the western boundary of 16°N section, and 3.11×10^6 m^3/s of eastward transport through the southern boundary of 117°E section.

Moreover, the potential densities at the average sill depth (2 181 m) in Area A (36.91 kg/m^3) and Area B (36.85 kg/m^3) are fairly consistent with *in situ* observations from Zhao et al. (2014). Along the Luzon Strait, the internal tides and waves over rough topography, such as seamounts, ridges and canyons, enhance the diapycnal mixing in the Luzon Strait by up to two orders larger than its counterpart in the North Pacific, consequently transforming well-stratified north Pacific deepwater into rather homogeneous SCS deepwater (Tian et al., 2009). As reported by Zhao et al. (2014), the observed potential density at the sill depth is 36.92 kg/m^3 in the upstream and 36.87 kg/m^3 in the downstream of the Luzon Strait. The consistency in the potential density between the GDEM-V3.0 and the observations (Zhao et al., 2014) increases our confidence in the quality of the GDEM-V3.0. We therefore believe that the GDEM-V3.0 is well suited for the present study.

3.2 *Relative importance of bifurcation depth and density difference*

Similar to the analysis described above, we calculate the potential density on the two sides of the Luzon Strait using the monthly climatology of the GDEM-V3.0 and seasonal climatology of the WOA13, and find that both the bifurcation depth and the density difference vary with time (Figs 3a and b). Figure 3a illustrates the bifurcation depth with two lower positions and two higher positions for both datasets, varying between 1 414 m and 1 525 m. A semiannual-like variability is revealed. The bifurcation depth in WOA13 peaks in fall (October–December), while that in the GDEM-V3.0 reaches its highest position in December. The bifurcation depth in the two datasets reaches its second highest position in spring (April–June) and June, respectively. Similarly, the bifurcation depth in the WOA13 is of lower positions in winter and summer, while that in the GDEM-V3.0 reaches its deepest positions in April and August. Hence, the thickness of the deepwater overflow, h_u=2 181 minus the bifurcation depth, is not a constant as assumed by previous studies, but is highly variable with season, which is expected to influence the seasonality of the deepwater overflow in the Luzon Strait.

The most notable feature of the density difference between the two sides of the Luzon Strait (Fig. 3b), a measure of the baroclinic pressure head, is its positive value all year round, which confirms a persistent deepwater overflow crossing the Luzon Strait sill from the western Pacific to the SCS. The enhanced diapycnal mixing in the Luzon Strait and the SCS is believed to be responsible for the density difference (Qu et al., 2006; Tian et al., 2009). Other features of the density difference include: (1) the relatively smaller density difference in winter and spring in the WOA13 and (2) the relatively larger density difference with little variability throughout the year in the GDEM-V3.0. The causes for these differences between the two datasets are not known. They could result in part from the limited availability of observations.

On the basis of the GDEM-V3.0, the shallowest and deepest bifurcations of the year take place at 1 414 m in December and 1 478 m in April. The corresponding h_u is 767 m in December and 703 m in April. Considering the role of h_u raised to a power (Whitehead, 1989, 1998), the ratio of the transport induced by h_u equals 767^2/703^2=119%. In other words, the maximum monthly transport is 19% greater than the minimum monthly transport induced by changes in the bifurcation depth. In contrast, as shown in Fig. 3b, the greatest density difference is 0.065 3 kg/m^3 in August, and the smallest density difference is 0.064 45 kg/m^3 in January. The corresponding ratio of transport induced by the density difference is 0.065 3/0.064 45=101.3%. This shows the maximum transport is 1.3% greater than the minimum transport induced by changes in the density difference. Therefore, the variability of the transport induced by the thickness of the overflow is significantly greater than that induced by the density difference between the two sides of the Luzon Strait.

On the other hand, the variability in the thickness of the deepwater overflow and the density difference between the two sides of the Luzon Strait in the WOA13 is greater than that in GDEM-V3.0. Among the four seasons, the greatest h_u (761 m) occurs in fall, and the smallest (656 m) in summer. The ratio of the volume transport induced by variable h_u is 761^2/656^2=134%, while the ratio of the greatest (0.064 6 kg/m^3 in summer) to the smallest (0.055 2 kg/m^3 in winter) density difference is 117%. It confirms again that the variable h_u induces a larger seasonal variability than the density difference does. In other words, both datasets indicate that the bifurcation depth is a more important factor influencing the seasonal variability of the deepwater overflow. Ig-

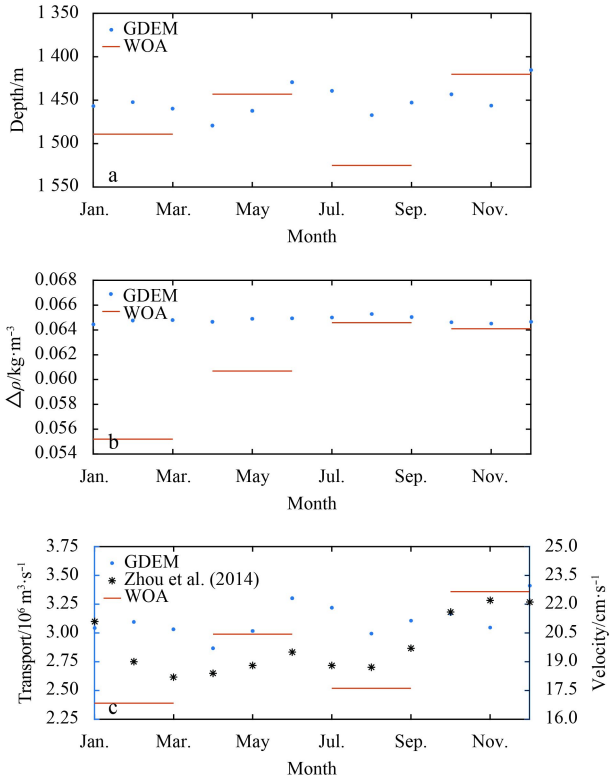

Fig. 3. Seasonal cycle of the bifurcation depth (a) and the difference of potential density (kg/m^3) between Areas A and B at 2 181 m (b), and deepwater overflow transport (blue dots for the GDEM and red lines for the WOA) estimated from Eq. (1) and the monthly climatology of the along Bashi Channel velocity from observations (asterisks) reported by Zhou et al. (2014) (c).

noring this factor will lead to incorrect conclusions.

3.3 *Seasonal variability of deepwater overflow*

The seasonal climatology of the deepwater overflow transport is calculated from Eq. (1), based on the seasonally variable bifurcation depth (Fig. 3a) and the density difference (Fig. 3b). The result illustrates a similar variability to the bifurcation depth (Fig. 3c), but differs from that of the density difference. Again, it suggests that the thickness of the overflow is the more important factor influencing the deepwater overflow, while the density difference is relatively minor based on the existing datasets we have used.

Similar to the bifurcation depth, the most notable feature of the deepwater overflow is the semiannual-like variability derived from both WOA13 and GDEM-V3.0. The overflow derived from the WOA13 is weaker in winter and summer, and stronger in spring and fall. Likewise, the monthly climatology of the deepwater overflow derived from the GDEM-V3.0 represents a rather distinct semiannual variability throughout the year: with two minima in April (2.87×10^6 m^3/s) and August (3.0×10^6 m^3/s) and two maxima in December (3.4×10^6 m^3/s) and June (3.3×10^6 m^3/s). The seasonal climatology of both datasets reveals the strongest Luzon Strait overflow occurring in fall and the weakest in winter or early spring, which has never been reported by previous numerical modeling studies. As a convincing evidence, this seasonal variability of deepwater overflow is coincident with the monthly climatology of velocity along the deep Bashi Channel reported by Zhou et al. (2014) based on the 3.5 a continuous *in situ* observation (Fig. 3c). This observed along-channel velocity, which is the longest existing time series in the Luzon Strait, also demonstrates a semiannual-like variability, with the weakest velocity occurring in March and August and the strongest velocity occurring in November–December and June. It substantially confirms our estimate of the deepwater overflow derived from the hydraulic theory. So, according to all these observations, the Luzon Strait deepwater overflow can be more likely classified as a weak semiannual variability. It is not as simply as being addressed stronger in one season and weaker in the opposite season by the previous studies based on numerical simulations.

3.4 *Influence of deepwater overflow on the deep SCS circulation*

To examine the influence of varying deepwater overflow on the deep circulation pattern, we use the thermal wind relation to calculate the geostrophic velocity (e.g., Stommel and Arons, 1959–1960). The sensitivity of the geostrophic velocity to the selection of a no-motion reference level has been discussed by previous studies (e.g., Qu et al., 1998; Wang et al., 2011). In this study, the no-motion reference level is chosen at depths of 1 500 m and 2 400 m, respectively, in the two cases of the calculation. The former corresponds to the climatological mean bifurcation depth, and the latter is just below the deepest sill of the Luzon Strait. Though there are some discrepancies between these two cases of no-motion reference level, the overall circulation patterns are similar. Figure 4 illustrates the depth averaged currents below 2 400 m in April, June, August and December, with the no-motion reference level at 1 500 m based on the GDEM-V3.0. Owing to the similarity, we do not show the depth averaged currents with the no-motion reference level at 2 400 m. The geostrophic currents in the deep SCS Basin characterize that the deepwater overflow spreads away from west of the Luzon Strait, turns northwestward/southwestward off the southern China continental slope, intensifies along the western boundary of the deep basin, and eventually forms a basin-wide cyclonic circulation (e.g., Qu et al., 2006; Wang et al., 2011). Obviously, Fig. 4 does not show any significant seasonal variability in the deep circulation of the SCS, even though the circulation patterns of April and August (Figs 4a and c) correspond to the weakest overflow and those of June and December (Figs 4b and d) correspond to the strongest

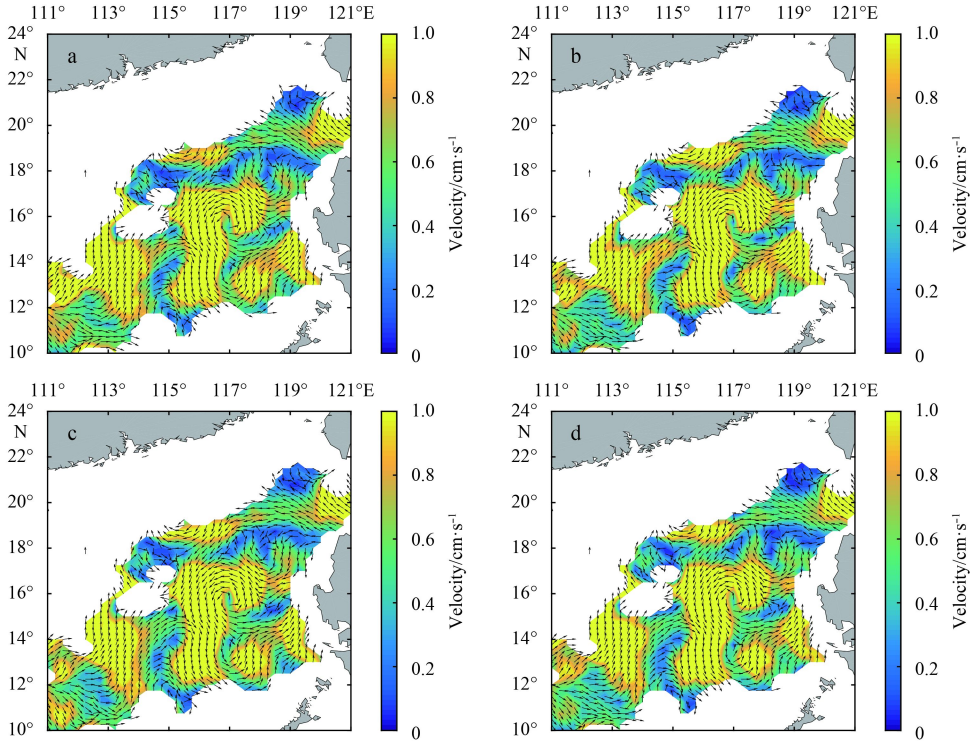

Fig. 4. Depth averaged velocity below 2 400 m in the SCS based on the GDEM-V3.0 in April (a), June (b), August (c), and December (d) with the no-motion reference level at 1 500 m. The color bar depicts the strength of velocity.

overflow in the Luzon Strait. The reason probably lies in the fact that the seasonal variability of the Luzon Strait deepwater overflow is relatively weak. On the other hand, it may take some time for dense Pacific water to form a possible cyclonic circulation in the deep SCS Basin (Qu et al., 2006; Wang et al., 2011; Zhu et al., 2016). Therefore, one may have reasons to expect a phase-lag between changes in the Luzon Strait deepwater overflow and changes in the SCS circulation. The formation and adjustment of the deep circulation also depend on waves in the deep SCS Basin, which need to be investigated by separate studies in the future when observations in the deep SCS are available.

The WOA13 dataset shows a rather different and irregular deep circulation pattern below 2 400 m in Fig. 5. This seasonal circulation pattern truly reflects the fact that observations in the vast deep basin of the SCS are sparse. With only tens of temperature and salinity profiles at the depth of 3 500 m or below, the seasonal circulation pattern does not construct a "regularly" cyclonic gyre as the GDEM-V3.0 model output does in the deep SCS. Some "certain" messages we can obtain from these charts include the spreading overflow away from west of the Luzon Strait, the irregularly cyclonic gyre in the central basin in winter and spring, and a cyclonic circulation at the southwest end of the basin. The weakest circulation pattern does not occur in winter to correspond to the weakest overflow in the Luzon Strait. Similarly, the strongest circulation pattern does not occur in fall to correspond to the strongest overflow. Instead, the deep circulation in fall is the weakest among the four seasons throughout the year. These results further consolidate the opinion that the seasonal mean circulation pattern in the deep SCS does not respond synchronously to the seasonality of the deepwater overflow in the Luzon Strait.

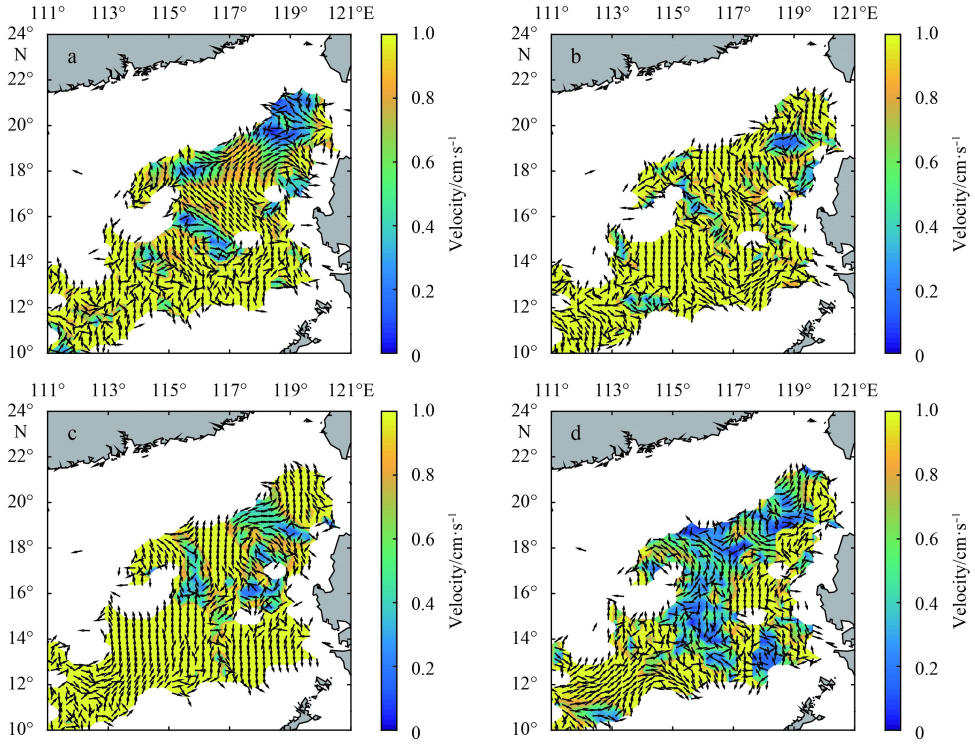

Fig. 5. Depth averaged velocity below 2 400 m in the SCS based on the WOA13 in winter (January–March) (a), spring (April–June) (b), summer (July–September) (c), and fall (October–December) (d) with the no-motion reference level at 1 500 m. The color bar depicts the strength of velocity.

4 Summary and discussion

Our analysis based on the WOA13 and GDEM-V3.0 datasets confirms the existence of an all year-round density difference between the two sides of the deep Luzon Strait, which is responsible for the persistent deepwater overflow from the western Pacific into the SCS. The seasonal variation in this density difference was believed to play a leading role in modulating the Luzon Strait deepwater overflow. But, our analysis shows that the seasonal varying bifurcation depth plays a more important role in generating the seasonal variability of the deepwater overflow. Ignoring the seasonal variation of the bifurcation depth would lead to inaccurate estimate of the deepwater overflow. For example, Zhou et al. (2014) detected a seasonal maximum in fall and a seasonal minimum in spring in velocity of the deepwater overflow, which is inconsistent with the seasonal variability of the density difference. Our results indicate that the deepwater overflow reaches its seasonal maximum in December (3.4×10^6 m^3/s, GDEM-V3.0) or in October–December (3.36×10^6 m^3/s, WOA13), with two maxima and minima presenting a semiannual-like variability. This weak semiannual variability is consistent with the monthly climatology of the longest (3.5 a) observed velocity in the Bashi Channel, the major deepwater pathway in the Luzon Strait. The deepwater overflow is relatively weak in the other seasons, with its seasonal minimum occurring in winter (2.39×10^6 m^3/s, WOA13) or in April (2.87×10^6 m^3/s, GDEM-V3.0). Neither GDEM-V3.0 nor WOA13 shows evidence for a good correspondence between the seasonal circulation pattern in the deep SCS Basin and the seasonal variability of the deepwater overflow in the Luzon Strait. In fact, since it takes time for the dense Pacific water to pass through the Luzon Strait and possibly form a cyclonic circulation in the deep SCS Basin, we believe that a certain period of time-lag between the two is reasonable. But, how long

this time-lag is remains unknown, and this needs to be investigated further by research as observations in the deep SCS become available.

In general, the hydraulic theory provides an upper bound estimate of the deepwater overflow, since it ignores the complex bathymetry, overlying flow, and friction (e.g., Qu and Song, 2009). The ratio of hydraulic estimation to direct observation ranges from 1.0 to 2.7 according to a previous study by Whitehead (1998). Likewise, the deepwater overflow in the Luzon Strait is significantly overestimated by the hydraulic theory, compared with those from the direct observations of Zhou et al. (2014) and Zhao et al. (2014). Nevertheless, the main features, including the weak semiannual variability, are consistent with the monthly climatology of the along-channel velocity reported by Zhou et al. (2014).

A complete understanding of the hydraulic theory with its application to the Luzon Strait based on the GDEM-V3.0 and WOA13 datasets appears to confer some insight into the seasonality of the deepwater overflow. How temperature and salinity in the deep ocean respond to the surface wind and heat flux is unknown. Why the deepwater overflow is of maximum thickness in December or late fall and how this variability is related to adjacent water in the western Pacific require further investigation. Our preliminary result shows that the stronger deepwater overflow is always accompanied by lower potential temperature of the deepwater on the Pacific side of the Luzon Strait, while the weaker deepwater overflow always concurs with higher potential temperature, as shown in Fig. 6. This result was derived from the WOA13 and the GDEM-V3.0 and verified by the *in situ* observation of Zhou et al. (2014), but it has never been reported by previous studies. A lower temperature on the Pacific side of the Luzon Strait may result in a higher density in the deep water. As a result of enhanced diapycnal mixing, water on the SCS side of the Luzon Strait is relatively homogeneous. Thus, a higher density of deepwater on the Pacific side means a stronger baroclinic pressure head driving force with the greater thickness of the deepwater overflow, which generates the strongest deepwater overflow of the year.

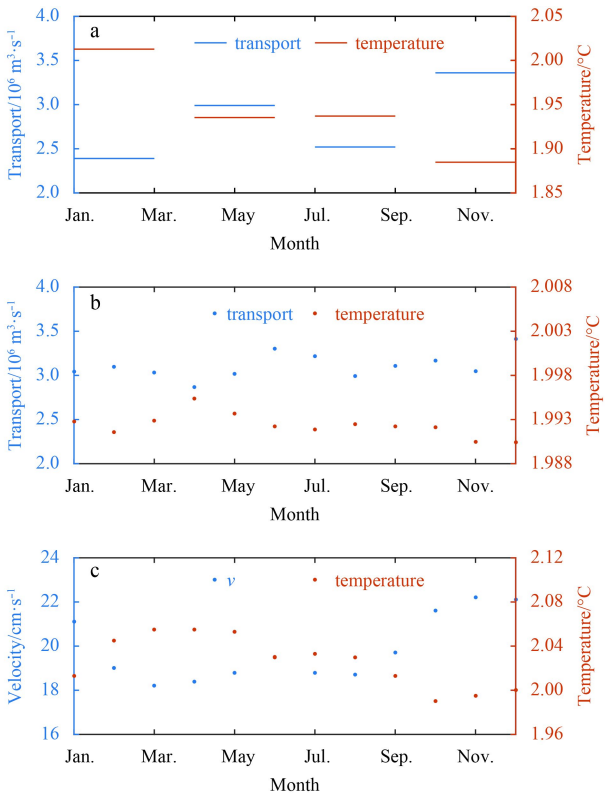

Fig. 6. The relationship between the deepwater overflow in the Luzon Strait and the potential temperature (°C) at depth of 2 000 m in Area A, based on WOA13 (a), GDEM-V3.0 (b), and relationship between the along-channel velocity and the potential temperature (°C) in the Bashi Channel reported by Zhou et al. (2014) (c).

References

Boyer T P, Garcia H E, Locarnini R A, et al. 2014. 2013 world ocean atlas aids high-resolution climate studies. Eos, 95(41): 369–370

Carnes M R. 2009. Description and Evaluation of GDEM-V3.0, Tech Rep NRL/MR/7330–09–9165. Washington, D C. Nav Res Lab, 21.

Fang Guohong, Wang Yonggang, Wei Zexun, et al. 2009. Interocean circulation and heat and freshwater budgets of the South China Sea based on a numerical model. Dyn Atmos Oceans, 47(1–3): 55–72

Lan Jian, Wang Yu, Cui Fengjuan, et al. 2015. Seasonal variation in the South China Sea deep circulation. J Geophys Res: Oceans, 120(3): 1682–1690, doi: 10.1002/2014JC010413

Nitani H. 1972. Beginning of the Kuroshio. In: Stommel H, Yashida K, eds. Kuroshio: Physical Aspects of the Japan Current. Seattle: University of Washington Press, 129–163

Qu Tangdong, Girton J B, Whitehead J A. 2006. Deepwater overflow through Luzon Strait. J Geophys Res, 111(C1): C01002, doi: 10.1029/2005JC003139

Qu Tangdong, Mitsudera H, Yamagata T. 1998. On the western boundary currents in the Philippine Sea. J Geophys Res, 103(C4): 7537–7548

Qu Tangdong, Mitsudera H, Yamagata T. 2000. Intrusion of the North Pacific waters into the South China Sea. J Geophys Res, 105(C3): 6415–6424

Qu Tangdong, Song Y T, Yamagata T. 2009. An introduction to the South China Sea throughflow: its dynamics, variability, and application for climate. Dyn Atmos Oceans, 47(1–3): 3–14, doi: 10.1016/j.dynatmoce.2008.05.001

Smith W H F, Sandwell D T. 1997. Global sea floor topography from satellite altimetry and ship depth soundings. Science, 277(5334): 1956–1962

Stommel H, Arons A B. 1959–1960. On the abyssal circulation of the world ocean—II. An idealized model of the circulation pattern and amplitude in oceanic basins. Deep-Sea Res (1953), 6: 217–233

Teague W J, Carron M J, Hogan P J. 1990. A comparison between the generalized digital environmental model and Levitus climatologies. J Geophys Res, 95(C5): 7167–7183

Tian Jiwei, Yang Qingxuan, Liang Xinfeng, et al. 2006. Observation of Luzon Strait transport. Geophys Res Lett, 33(19): L19607, doi: 10.1029/2006GL026272

Tian Jiwei, Yang Qingxuan, Zhao Wei. 2009. Enhanced diapycnal mixing in the South China Sea. J Phys Oceanogr, 39: 3191–3203, doi: 10.1175/2009jpo3899.1

Wang Joe. 1986. Observation of abyssal flows in the northern South China Sea. Acta Oceanogr Taiwan, 16: 36–45

Wang Guihua, Xie Shangping, Qu Tangdong, et al. 2011. Deep South China Sea circulation. Geophys Res Lett, 38(5): L05601, doi: 10.1029/2010GL046626

Whitehead J A. 1989. Internal hydraulic control in rotating fluids—applications to oceans. Geophys Astrophys Fluid Dyn, 48(1–3): 169–192

Whitehead J A. 1998. Topographic control of oceanic flows in deep passages and straits. Rev Geophys, 36(3): 423–440, doi: 10.1029/98RG01014

Wyrtki K. 1961. Physical Oceanography of the Southeast Asian Waters, Naga Rep 2. Scripps Inst of Oceanogr, 195

Xie Qiang, Xiao Jin'gen, Wang Dongxiao, et al. 2013. Analysis of deep-layer and bottom circulations in the South China Sea based on eight quasi-global ocean model outputs. Chin Sci Bull, 58(32):

4000–4011, doi: 10.1007/s11434–013-5791–5

Xu Fanghua, Oey L Y. 2014. State analysis using the local ensemble transform Kalman Filter (LETKF) and the three-layer circulation structure of the Luzon Strait and the South China Sea. Ocean Dyn, 64(6): 905–923, doi: 10.1007/s10236–014-0720-y

Yang Qingxuan, Tian Jiwei, Zhao Wei. 2010. Observation of Luzon Strait transport in summer 2007. Deep-Sea Res: I. Oceanogr Res Pap, 57(5): 670–676

Zhang Zhengguang, Zhao Wei, Liu Qinyu. 2010. Sub-seasonal variability of Luzon Strait transport in a high resolution global model. Acta Oceanologica Sinica, 29(3): 9–17, doi: 10.1007/s13131–010-0032–0

Zhang Zhiwei, Zhao Wei, Tian Jiwei, et al. 2015. Spatial structure and temporal variability of the zonal flow in the Luzon Strait. J Geophys Res: Oceans, 120(2): 759–776, doi: 10.1002/2014JC010308

Zhao Wei, Zhou Chun, Tian Jiwei, et al. 2014. Deep water circulation in the Luzon Strait. J Geophys Res: Oceans, 119(2): 790–804, doi: 10.1002/2013JC009587

Zhou Chun, Zhao Wei, Tian Jiwei, et al. 2014. Variability of the deep-water overflow in the Luzon Strait. J Phys Oceanogr, 44(11): 2972–2986

Zhu Yaohua, Fang Guohong, Wei Zexun, et al. 2016. Seasonal variability of the meridional overturning circulation in the South China Sea and its connection with inter-ocean transport based on SODA2.2.4. J Geophys Res: Oceans, 121(5): 3090–3105, doi: 10.1002/2015JC011443